



A LETTERS JOURNAL EXPLORING
THE FRONTIERS OF PHYSICS

OFFPRINT

**Helicity in cylindrically confined Yukawa
systems**

E. C. OĞUZ, R. MESSINA and H. LÖWEN

EPL, 94 (2011) 28005

Please visit the new website
www.epljournal.org

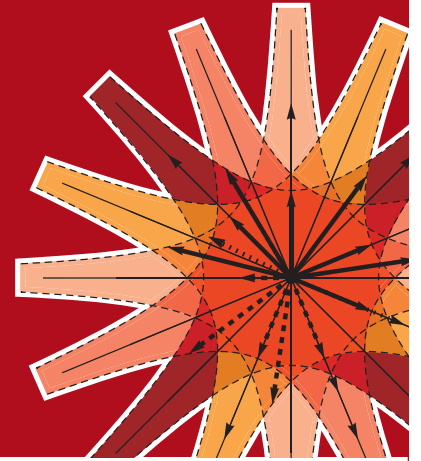


epl

A LETTERS JOURNAL
EXPLORING THE FRONTIERS
OF PHYSICS

The Editorial Board invites you
to submit your letters to EPL

www.epljournal.org



Six good reasons to publish with EPL

We want to work with you to help gain recognition for your high-quality work through worldwide visibility and high citations. As an EPL author, you will benefit from:

- 1 Quality** – The 40+ Co-Editors, who are experts in their fields, oversee the entire peer-review process, from selection of the referees to making all final acceptance decisions
- 2 Impact Factor** – The 2009 Impact Factor increased by 31% to 2.893; your work will be in the right place to be cited by your peers
- 3 Speed of processing** – We aim to provide you with a quick and efficient service; the median time from acceptance to online publication is 30 days
- 4 High visibility** – All articles are free to read for 30 days from online publication date
- 5 International reach** – Over 2,000 institutions have access to EPL, enabling your work to be read by your peers in 100 countries
- 6 Open Access** – Experimental and theoretical high-energy particle physics articles are currently open access at no charge to the author. All other articles are offered open access for a one-off author payment (€1,000)

Details on preparing, submitting and tracking the progress of your manuscript from submission to acceptance are available on the EPL submission website www.epletters.net

If you would like further information about our author service or EPL in general, please visit www.epljournal.org or e-mail us at info@epljournal.org



IOP Publishing

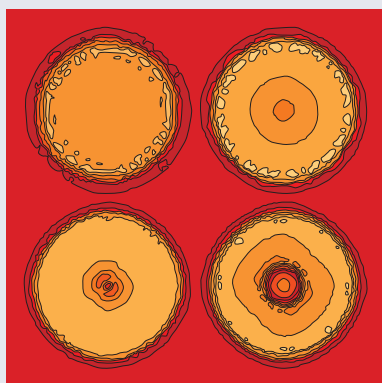
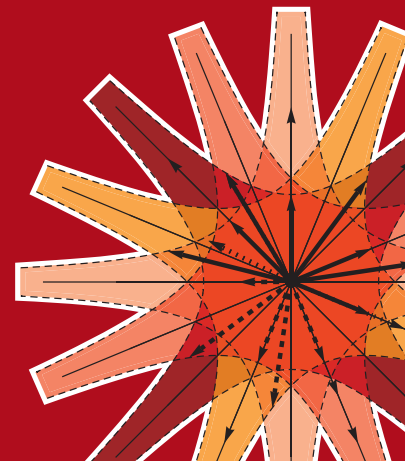
Image: Ornamental multiplication of space-time figures of temperature transformation rules
(adapted from T. S. Biró and P. Ván 2010 *EPL* **89** 30001; artistic impression by Frédérique Swist).



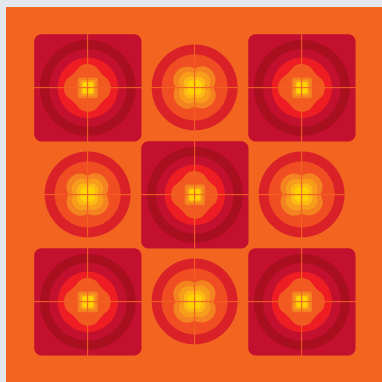
A LETTERS JOURNAL
EXPLORING THE FRONTIERS
OF PHYSICS

EPL Compilation Index

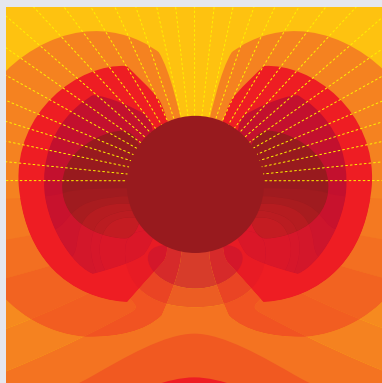
www.epljournal.org



Biaxial strain on lens-shaped quantum rings of different inner radii, adapted from **Zhang et al** 2008 *EPL* **83** 67004.



Artistic impression of electrostatic particle-particle interactions in dielectrophoresis, adapted from **N Aubry and P Singh** 2006 *EPL* **74** 623.



Artistic impression of velocity and normal stress profiles around a sphere that moves through a polymer solution, adapted from **R Tuinier, J K G Dhont and T-H Fan** 2006 *EPL* **75** 929.

Visit the EPL website to read the latest articles published in cutting-edge fields of research from across the whole of physics.

Each compilation is led by its own Co-Editor, who is a leading scientist in that field, and who is responsible for overseeing the review process, selecting referees and making publication decisions for every manuscript.

- Graphene
- Liquid Crystals
- High Transition Temperature Superconductors
- Quantum Information Processing & Communication
- Biological & Soft Matter Physics
- Atomic, Molecular & Optical Physics
- Bose-Einstein Condensates & Ultracold Gases
- Metamaterials, Nanostructures & Magnetic Materials
- Mathematical Methods
- Physics of Gases, Plasmas & Electric Fields
- High Energy Nuclear Physics

If you are working on research in any of these areas, the Co-Editors would be delighted to receive your submission. Articles should be submitted via the automated manuscript system at www.epletters.net

If you would like further information about our author service or EPL in general, please visit www.epljournal.org or e-mail us at info@epljournal.org



IOP Publishing

Image: Ornamental multiplication of space-time figures of temperature transformation rules (adapted from T. S. Bíró and P. Ván 2010 *EPL* **89** 30001; artistic impression by Frédérique Swist).

Helicity in cylindrically confined Yukawa systems

E. C. OĞUZ^(a), R. MESSINA and H. LÖWEN

*Institut für Theoretische Physik II: Weiche Materie, Heinrich-Heine-Universität Düsseldorf
Universitätsstraße 1, D-40225 Düsseldorf, Germany, EU*

received 1 February 2011; accepted in final form 16 March 2011

published online 15 April 2011

PACS 82.70.Dd – Colloids

PACS 64.70.K- – Solid-solid transitions

Abstract – By lattice sum minimization, we predict the ground state of particles interacting via a Yukawa potential which are confined in a quasi-one-dimensional cylindrical tube. As a function of screening strength and particle density, the zero-temperature phase diagram exhibits a cascade of stable crystals with both helical and non-helical structures. These quasi-one-dimensional crystals can be confirmed in experiments on confined charged colloidal suspensions, trapped dusty plasmas or ions in nanotubes.

Copyright © EPLA, 2011

Understanding the origin of helical structures in nature is of basic importance given the fact that many biomolecules (such as DNA [1]) and inner cell structures are helical. More specifically, if particles are confined to narrow cylinders under high pressure they will spontaneously assemble into helical structures [2–5]. This has been rationalized by considering a simple model of hard spheres in cylindrical tubes where the close-packed configurations have been analyzed and indeed show helical structures [6]. Furthermore, dipolar colloidal particles [7] and thermoresponsive microspheres [5] have been shown to self-organize into chiral aggregates and C₆₀ molecules [8–10] as well as polymers [11–13] confined to nanotubes exhibit spiral-like structures. Understanding the details of this pattern formation bears a high technological potential as photonic band gap fibers can be formed in cylindrical geometry [14,15] and colloidal nanowires with novel electrical properties may be fabricated out of helical structures. Moreover, helical colloidal clusters itself can further serve as “super”-molecules [7] which in solution self-assemble into fascinating novel liquid crystalline phases [16].

In this letter, we consider charged particles in hard cylindrical confinement interacting via a Yukawa pair potential. Thereby we generalize the hard-sphere model studied previously in ref. [6] towards finite screening lengths. By lattice sum minimization we obtain the ground state (at zero temperature) and predict a cascade of different helical and non-helical structures as a function of screening strength and particle density. In contrast to the hard-sphere case, some phases disappear at small

screening and re-entrant transitions show up. Our model is realized for charged colloidal suspensions under cylindrical confinement (cf. [17–26]), for trapped dusty plasmas [27,28] and for charged supramolecular aggregates or molecular ions in nanotubes [29–31]. We also remark that microspheres explored in [5] are governed by soft interactions such that our work here might be relevant for the findings in ref. [5].

In our model, we consider point-like particles interacting *via* the Yukawa pair-potential

$$V(r) = V_0 \frac{e^{-\kappa r}}{\kappa r}, \quad (1)$$

where r is the interparticle distance, $1/\kappa$ the screening length, and V_0 denotes an energy amplitude. N particles are confined inside a hard cylindrical tube of radius a and length L along the z -direction. At zero temperature, for a given reduced line density $\eta = Na/L$, the system will minimize its total potential energy per length L and the resulting optimal structure will only depend on the reduced inverse screening length $\lambda = \kappa a$. By varying λ , one interpolates between the unscreened Coulomb limit ($\lambda \rightarrow 0$) and the hard-sphere limit¹ ($\lambda \rightarrow \infty$) where the interaction is getting discontinuous.

At zero temperature and at given density η and reduced screening length λ , we have performed lattice sum minimizations for a broad set of candidate structures including

¹Note that in our model we have point-like particles. Nevertheless, at infinite screening ($\lambda \rightarrow \infty$), by taking an effective hard-core diameter corresponding to the smallest lattice constant, one expects to recover the phase behavior of hard spheres.

^(a)E-mail: ecoguz@thphy.uni-duesseldorf.de

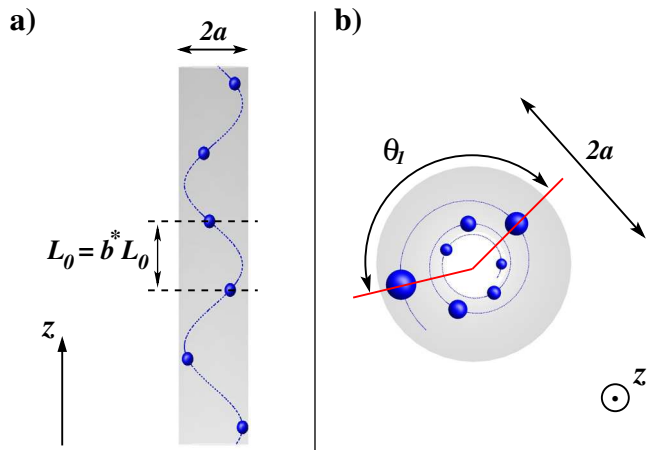


Fig. 1: (Color online) Schematic illustration of cylindrically confined particles in side (a) and top (b) view. The cylinder is shadowed and has a radius of $2a$. A helical phase structure is sketched. In (a) the dashed lines indicate the primitive cell of height L_0 . Here, we have $n=1$ such that the order parameter b^* equals 1. In the top view (b), the torsion angle θ_1 between two primitive cells is shown.

helical ones. A candidate possesses a unit cell containing $n \leq 6$ particles inside a cylindrical cavity which is then periodically replicated along the z -direction by a joint translation about L_0 along the z -axis (see fig. 1(a)) and rotation about a torsion angle θ around the z -axis. We restrict ourselves to $0 \leq \theta \leq \pi$ selecting one special chirality (note that opposite chirality leads to the same energy). Thus, a most general unit cell with $n=6$ can contain multiple primitive cells with $n=1, 2, 3$, resulting in the same phase structure. However, the corresponding torsion angles might differ. To distinguish between them we denote the n -dependence of the torsion angle explicitly and refer them as θ_n in general (see fig. 1(b)). There are two classes of structures, namely *non-helical* ones which by definition are torsion-free, *i.e.* they can be generated with a vanishing torsion angle $\theta_n = 0$, or *helical* ones which necessarily involve a non-vanishing one. Nevertheless, some special non-helical structures with $\theta_n = 0$ can also be generated with a finite torsion angle albeit with a different n .

The minimization of the total potential energy per particle is performed with respect to the positions of the n particles in the unit cell and the torsion angle while $L_0 = na/\eta$ is prescribed by the fixed line density η . First we classify the resulting structures into helical and non-helical ones. Next, in case a helical structure is degenerated with respect to different n , we select from all the possible structures the one with the smallest n . For the non-helical structures, we select the structure with the smallest n as well, which also satisfies a vanishing torsion angle. To characterize the height distribution of the particles in the unit cell, we assign, for each structure, a dimensionless order parameter $b^* = n \min_{i \neq j} \{|z_i - z_j|/L_0\}$, which describes

the smallest (reduced) interparticle distances among all distinct particle pairs (i, j) along the z -direction.

We explore the stability phase diagram in the regime $\lambda = 0.5, \dots, 100$ for $0 < \eta \leq 2.2$. The results are shown in fig. 2. Three helical structures $H1, H2, H3$ are stable which are labelled according to their (minimal) number of particles per unit cell while H stands for ‘‘helical’’. Besides three stable non-helical structures $N2, N4, N6$ set in. All these non-helical structures Nn (with $n=2, 4, 6$) can also be generated by a non-vanishing torsion angle θ_n with smaller unit cell number $n=1, 2, 3$ as compared to that corresponding to the torsion-free generation. Details are summarized in table 1 where also the corresponding values of the order parameters b^* and θ_6 are given. For instance, for the $H1$ structure, $b^* = 1$ while for $H2$ and $H3$, $0 < b^* < 1$. The non-helical phase $N2$ has a zigzag arrangement which can also be considered as a helix with $\theta_1 = \pi$ and $b^* = 1$. For the non-helical phase $N2$ ($N4$), each two (three) particles in the same unit cell possess the same z -coordinate. Furthermore, the non-helical ‘‘doublets’’ (‘‘triplets’’) of $N4$ ($N6$) are generated with a torsion angle $\theta_6 = \pi/2$ ($\theta_6 = 0$) with $b^* = 0$. In case of $N6$ θ_6 can also be chosen as $2\pi/3$, which yields the same phase. In all phases, all particles are located on the cylindrical surface although this was not assumed *a priori*. At higher densities, this will no longer be true in general.

Let us now discuss in greater depth the ground state phase diagram in the $\eta\lambda$ -plane (fig. 2). For large λ , we recover the stability sequence put forward for hard spheres in cylindrical confinement in ref. [6], namely

$$N2 \rightarrow H1 \rightarrow H2 \rightarrow N4 \rightarrow H2 \rightarrow H1 \\ \rightarrow H2 \rightarrow H3 \rightarrow N6, \quad (2)$$

for increasing density η . On the other hand, the opposite Coulomb limit $\lambda \rightarrow 0$ corresponding to unscreened ions in a cylinder, has not been considered before. Here we find the stability sequence

$$N2 \rightarrow H1 \rightarrow N4 \rightarrow H1 \rightarrow H2 \rightarrow N4,$$

i.e. the phases $H3$ and $N6$ vanish and the stability domain of $H2$ shrinks to a single point at $\eta = 1.50$. This implies that non-helical phases are preferred for the Coulomb limit (relative to the hard-sphere case). This general trend can be intuitively expected since the long-ranged Coulomb potential prefers more isotropic structures than the hard-sphere interaction which considers local packing constraints.

Interpolating between these two extremes at finite λ , the phase behavior is not just a simple interpolation but exhibits interesting re-entrance effects, which are indicated by the vertical and the horizontal arrow in fig. 2. For increasing λ , the $H2$ phase is reentrant at about $1.68 < \eta < 1.74$. Another re-entrance effect occurs for the $N4$ phase upon increasing η at fixed $\lambda \approx 7$. This is in line with the general observation that confinement effects (or external fields in general) yield re-entrance [17].

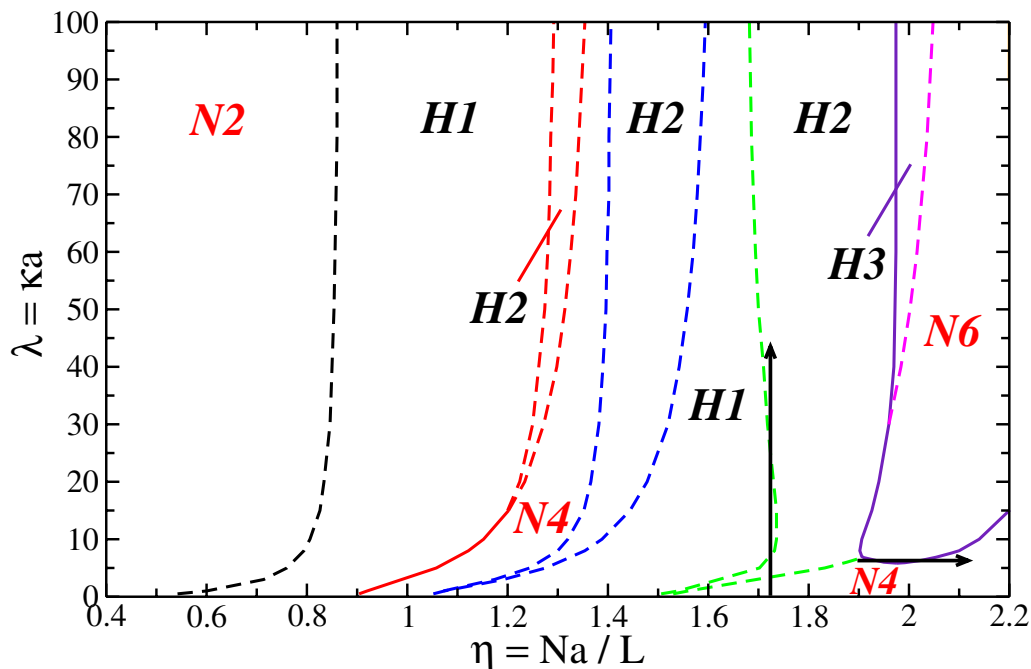


Fig. 2: (Color online) Zero-temperature phase diagram of a Yukawa system confined to a hard cylinder. As a function of screening strength λ and reduced density η , we obtain helical ($H1$, $H2$, $H3$) as well as non-helical ($N2$, $N4$, $N6$) phases. For $\lambda \rightarrow 0$, the stability domain of $H2$ shrinks to 0, while $H3$ ($N6$) already vanishes for $\lambda \lesssim 30$ ($\lambda \lesssim 7$). The dashed (full) lines indicate a 2nd-(1st-) order phase transition. The two arrows indicate the re-entrant transitions of $H2$ and $N4$.

Table 1: (Color online) Stable phase structures of the confined Yukawa system. The cylindrical confinement is illustrated by a gray tube of diameter $2a$. Two categories of stable phases are obtained: helical ($H1$, $H2$, $H3$) and non-helical ($N2$, $N4$, $N6$) phases. The helical geometry of $H1$, $H2$, and $H3$ is indicated by the helical lines connecting periodically repeated particles of the unit cell. Different particles of the unit cell are connected by different helices and are shown in different colors. For each phase, we show a top (upper) and a side (lower) view. Furthermore, possible values of b^* and θ_6 for each structure are also given. We also show the height of each primitive cell of helical phases as well as the height and the torsion angle of the torsion-free unit cell of the non-helical ones. Additionally, we show θ_3 for $N6$, for clarity.

$N2$	$H1$	$H2$	$N4$	$H3$	$N6$
$\theta_6 = 0$ $\theta_2 = 0$ $b^* = 1$	$0 < \theta_6 \leq \pi$ $b^* = 1$	$\pi/3 < \theta_6 < 2\pi/3$ $0 < b^* < 1$	$\theta_6 = \pi/2$ $\theta_4 = 0$ $b^* = 0$	$\pi/2 < \theta_6 < 2\pi/3$ $0 < b^* < 1/3$	$\theta_6 = 0$ (or $\theta_6 = 2\pi/3$) $\theta_3 = \pi/3$ $b^* = 0$

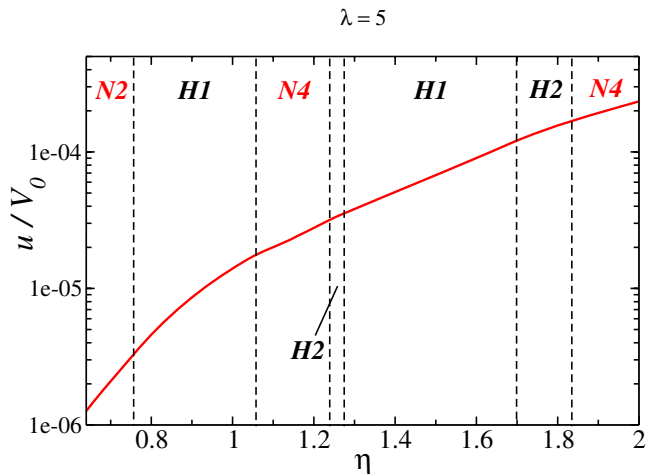


Fig. 3: (Color online) The static potential energy per particle u as a function of η for $\lambda = 5$.

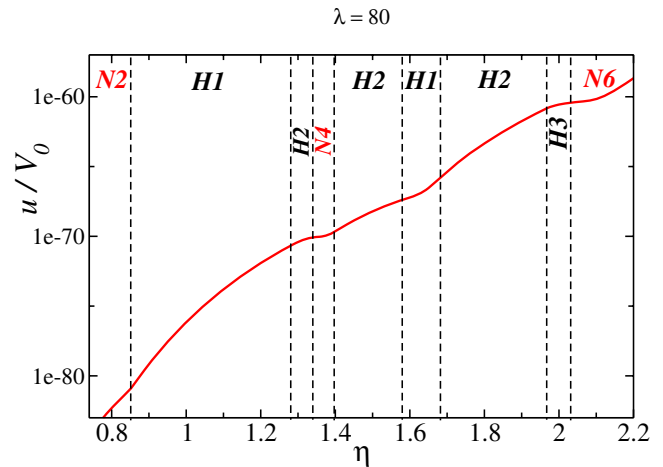


Fig. 5: (Color online) Same as fig. 3 for $\lambda = 80$.

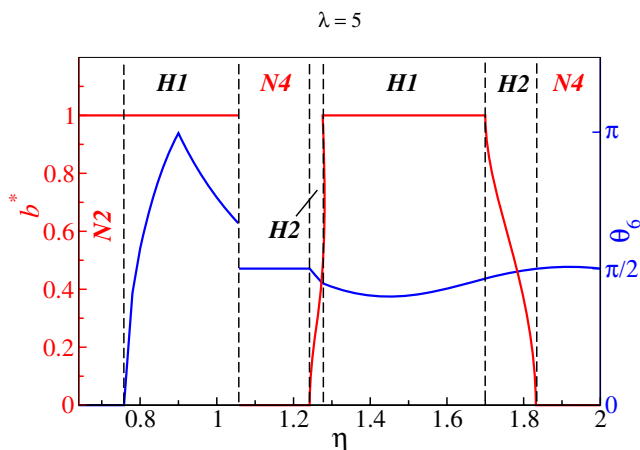


Fig. 4: (Color online) Order parameters b^* (red line) and θ_6 (blue line) for $\lambda = 5$ *vs.* η .

We remark that the re-entrance of solid phases resembles the isostructural solid-to-solid transition which occurs in three-dimensional square-well [32,33] and square-shoulder [34] systems. However, in the latter case, there is a true coexistence region between the two solids and a critical point shows up. Both features are absent here. Moreover, the pure Yukawa bulk system does not exhibit any re-entrance in the density-temperature plane, hence re-entrance is induced by confinement alone.

We finally address the order of the various solid-solid transitions in fig. 2 which results from the behavior of the energy per particle across the phase transition lines. Both, first-order and second-order transitions do occur and are indicated by solid and broken transition lines in fig. 2. This is captured by monitoring the energy per particle u and the order parameters b^* and θ_6 of the stable phase. These observables are plotted in figs. 3–6 as a function of η at two different λ . The cusps where $\theta_6 = \pi$ in the regime of $H1$ in figs. 4, 6 are due to the fact

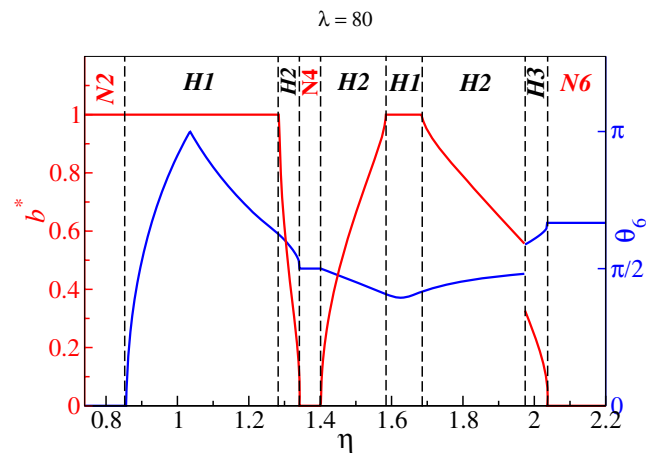


Fig. 6: (Color online) Same as fig. 4 for $\lambda = 80$. For the $N6$ phase, θ_6 is assumed to be $2\pi/3$ here since the second order of the $H3 \rightarrow N6$ becomes evident.

that we restrict the torsion angle to the interval $[0, \pi]$. Hence, the cusps are not indicating a phase boundary. In fact the energy is smooth at the cusps (see figs. 3, 5). The continuously non-differentiable points of the energy functions will indicate the first-order transitions. These points are revealed by the discontinuous jumps in b^* and θ_6 as a function of η while a continuous behavior implies a second-order transition (see figs. 4, 6).

In summary, we investigated the crystalline stability phase diagram of the cylindrically confined Yukawa particles at zero temperature. Our calculations yield several stable helical ($H1$, $H2$, $H3$) as well as non-helical phase structures ($N2$, $N4$, $N6$), where the integers denote the particles number in the corresponding unit cell. Within the density range considered here, we find that all particles are located on the surface of the cylinder. In the high screening regime, the stability cascade is given by eq. (2). In the plasma limit, on the other hand, the phases $H3$ and $N6$ are not stable anymore and the stability regime of the $H2$ phase shrinks to zero. Furthermore,

both first- as well as second-order phase transitions and a rich re-entrant behavior are found.

Future work should include the consideration of higher reduced densities. For finite screening $\lambda > 0$, this will yield structures with particles inside the cylinder. We further remark that for $\lambda = 0$ a homogeneously smeared opposite charge on the cylindrical surface will result in the same model as considered here since the inner electric field vanishes.

Since there is no strict phase transition in one-dimensional systems with short-ranged interactions for $T > 0$ [35,36], any finite temperature will smear out the solid-solid transitions found here leading to crossovers rather than strict discontinuities. The crossover behavior, however, can be very sharp in practice such that it is still useful to discriminate between phases.

In case we considered chiral structures in the present work, only one sign of chirality was presumed. However, in real biological systems, arrangements (*e.g.* helices) of two different signs of chirality could coincide, leading to a crossover between the both. Hence, this first-order transition will yield an interface region, which can be analyzed in a future work and the interface structure can be determined by given system parameters.

In order to study the stability of helical arrangements and non-helical crystals in a driven suspension, one could model a Poiseuille flow through the cylinder. The results could be compared to confined colloidal bilayers under shear [37]. Moreover, more complicated confining potentials like a combination of a parabolic potential [38] and a cylindrical hard void can be studied in the future.

We thank F. RAMIRO-MANZANO, A. MIJAILOVIĆ and T. PALBERG for helpful discussions. This work was supported by the DFG (SFB TR6, project D1).

REFERENCES

- [1] WATSON J. D. and CRICK F. H. C., *Nature*, **171** (1953) 737.
- [2] SNIR Y. and KAMIEN R. D., *Science*, **307** (2005) 1067.
- [3] ERICKSON R. O., *Science*, **181** (1973) 4101.
- [4] TYMCZENKO M., MARSAL L. F., TRIFONOV T., RODRIGUEZ I., RAMIRO-MANZANO F., PALLARES J., RODRIGUEZ A., ALCUBILLA R. and MESEGUER F., *Adv. Mater.*, **20** (2008) 2315.
- [5] LOHR M. A., ALSAYED A. M., CHEN B. G., ZHANG Z., KAMIEN R. D. and YODH A. G., *Phys. Rev. E*, **81** (2010) 040401.
- [6] PICKETT G. T., GROSS M. and OKUYAMA H., *Phys. Rev. Lett.*, **85** (2000) 3652.
- [7] ZERROUKI D., BAUDRY J., PINE D., CHAIKIN P. and BIBETTE J., *Nature*, **455** (2008) 380.
- [8] HODAK M. and GIRIFALCO L. A., *Phys. Rev. B*, **67** (2003) 075419.
- [9] MICKELSON W., ALONI S., HAN W.-Q., CUMINGS J. and ZETTL A., *Science*, **300** (2003) 467.
- [10] KHLOBYSTOV A. N., BRITZ D. A., ARDAVAN A. and BRIGGS G. A., *Phys. Rev. Lett.*, **92** (2004) 245507.
- [11] DOBRIYAL P., XIANG H., KAZUYUKI M., CHEN J.-T., JINNAI H. and RUSSELL T. P., *Macromolecules*, **42** (2009) 9082.
- [12] PETERCA M., PERCEC V., IMAM M. R., LEOWANAWAT P., MORIMITSU K. and HEINEY P. A., *J. Am. Chem. Soc.*, **130** (2008) 14840.
- [13] LINDNER J. P., ROSEN C., STUDER A., STASIAK M., RONGE R., GREINER A. and WENDORFF H.-J., *Angew. Chem., Int. Ed.*, **48** (2009) 8874.
- [14] BANDARU P. R., DARAIO C., YANG K. and RAO A. M., *J. Appl. Phys.*, **101** (2007) 094307.
- [15] YANG S. M., SOKOLOV I., COOMBS N., KRESGE C. T. and OZIN G. A., *Adv. Mater.*, **11** (1999).
- [16] WENSINK H. H. and JACKSON G., *J. Chem. Phys.*, **130** (2009) 234911.
- [17] MESSINA R. and LÖWEN H., *Phys. Rev. Lett.*, **91** (2003) 146101.
- [18] MESSINA R., *J. Phys.: Condens. Matter*, **21** (2009) 113102.
- [19] LÖWEN H., HÄRTEL A., BARREIRA-FONTECHA A., SCHÖPE H. J., ALLAHYAROV E. and PALBERG T., *J. Phys.: Condens. Matter*, **20** (2008) 404221.
- [20] OĞUZ E. C., MESSINA R. and LÖWEN H., *J. Phys.: Condens. Matter*, **21** (2009) 424110.
- [21] OĞUZ E. C., MESSINA R. and LÖWEN H., *EPL*, **86** (2009) 28002.
- [22] GRANDNER S. and KLAPP S. H. L., *EPL*, **90** (2010) 68004.
- [23] REINMÜLLER A., SCHÖPE H. J. and PALBERG T., *Soft Matter*, **6** (2010) 5312.
- [24] ERAL H. B., OH J. M., VAN DEN ENDE D., MUGELE F. and DUTTS M. H. G., *Langmuir*, **26** (2010) 16722.
- [25] ERAL H. B., VAN DEN ENDE D., MUGELE F. and DUTTS M. H. G., *Phys. Rev. E*, **80** (2009) 061403.
- [26] DÓNKO Z., KALMAN G. J. and HARTMANN P., *J. Phys.: Condens. Matter*, **20** (2008) 413101.
- [27] MORFILL G. E. and IVLEV A. V., *Rev. Mod. Phys.*, **81** (2009) 1353.
- [28] PIACENTE G., HAI G. Q. and PEETERS F. M., *Phys. Rev. B*, **81** (2010) 024108.
- [29] TORIMOTO T., TSUDA T., OKAZAKI K. and KUWABATA S., *Adv. Mater.*, **22** (2010) 1196.
- [30] ZHANG H. T., LI Y.-Z., WANG T. W., NFOR E. N., H.-Q. and YOU X.-Z., *Eur. J. Inorg. Chem.*, issue No. 17 (2006) 3532.
- [31] DZUBIELLA J., ALLEN R. J. and HANSEN J. P., *J. Chem. Phys.*, **120** (2004) 5001.
- [32] BOLHUIS P., HAGEN M. and FRENKEL D., *Phys. Rev. E*, **50** (1994) 4880.
- [33] LIKOS C. N., NÉMETH Z. T. and LÖWEN H., *J. Phys.: Condens. Matter*, **6** (1994) 10965.
- [34] BOLHUIS P. and FRENKEL D., *J. Phys.: Condens. Matter*, **9** (1997) 381.
- [35] VAN HOVE L., *Physica*, **16** (1950) 137.
- [36] CUESTA J. A. and SÁNCHEZ A., *J. Stat. Phys.*, **115** (2004) 869.
- [37] MESSINA R. and LÖWEN H., *Phys. Rev. E*, **73** (2006) 011405.
- [38] FERREIRA W. P., FARIAS G. A. and PEETERS F. M., *J. Phys.: Condens. Matter*, **22** (2010) 285103.